1-1-2010

Electroless Deposition Of Superconducting Magnesium Diboride Thin Films On Various Substrates

Khrupa Saagar Vijayaragavan
Wayne State University

ELECTROLESS DEPOSITION OF SUPERCONDUCTING MAGNESIUM DIBORIDE THIN FILMS ON VARIOUS SUBSTRATES

by

KHRUPA SAAGAR VIJAYARAGAVAN

THESIS

Submitted to the Graduate school

of Wayne State University,

Detroit, Michigan

in partial fulfillment of the requirements

for the degree of

MASTER OF SCIENCE

2010

MAJOR: CHEMICAL ENGINEERING

Approved By:

_____

Advisor Date

_____

Advisor Date

DEDICATION

This thesis is dedicated to my wonderful parents, Vijayaragavan and Subhashree who raised me to be the person I am today. I would like to thank my brother, sister-in-law, grandmother, my uncle, aunt and beloved cousins for being there through my good and bad times. Thank you for unconditional love, guidance, support that you have always given me, helping me succeed and instilling in me the required confidence. I also thank my closest friends that I am fortunate enough to have been blessed with.

ACKNOWLEDGMENTS

I am deeply indebted to my advisor Dr. Susil K Putatunda and co-advisor Dr. Gavin Lawes for their constant support. Without their help, this work would not be possible. I would like to thank my committee members to attend my thesis defense: Dr. Howard Matthew and Dr. Harpreet Singh. Their advice and patience is appreciated. I thank my department chair Dr. Charles Manke and Dr. Yinlung Huang for giving me a chance to participate in the department research activity. Many thanks to Dr. Ratna Naik for giving me permission and access to utilize laboratory facilities in Department of Physics and Astronomy

I must also acknowledge Mr. Ambesh Dixit, PhD student of Physics Department for his advice, science discussions and helping me obtain magnetic susceptibility data through SQUID measurements on my samples without whom my research would be incomplete. I gratefully thank Dr. Yi Liu for training and support on scanning electron microscope and Dr. Mary Jane Heeg for X-Ray diffractional analysis.

I would like to show my gratitude to my close and extended family members for providing a loving support. Also to my lab mates Abhijith, Abhilash, Codrick and Varun for friendly environment during laboratory work hours.

In conclusion I recognize that this research would not have been possible without the financial assistance of National Science Foundation (NSF) for our project. My gratitude to Dr Susil K Putatunda and my chair for providing me graduate teaching and research assistantship.

TABLE OF CONTENTS

LIST OF TABLES

LIST OF FIGURES

CHAPTER 1 – INTRODUCTION

1.1 – Introduction

Since 1960's researchers have explored the possibility that superconducting properties of thin films may be superior to or at least different from those of bulk materials. A number of techniques have been developed for synthesizing superconducting thin film including electrochemical synthesis [1]; electrophoresis based techniques [2], sol-gel synthesis [3], molecular beam epitaxy [4], ion beam synthesis [5], and pulsed laser deposition [6], among others. These techniques have several limitations such as requiring high temperatures and high pressures, possibly producing non uniform coatings, and result in high processing costs. They also require complex equipment such as vacuum deposition chamber, ion implant chamber, electrode assemblies etc, or are only suitable for producing thin films on certain types of conductive substrates as in case of electrochemical synthesis. Electroless Plating is an effective alternate technique for preparing superconducting thin films on diverse substrates having irregular shape and size. Electroless plating typically uses a redox reaction to deposit metals on surfaces without requiring an electric current [8, 9]. The technique of electroless plating addresses some of the processing shortcomings of these other deposition processes like limitations on the substrate size and geometry, energy consumption and cost. To date, this technique has been almost universally employed only for the deposition of elemental metals.

In recent years there has been significant interest in preparing superconducting thin films of magnesium diboride (MgB_2). Its relatively high critical temperature of 39 K, large critical field, coherence length, magnetic penetration depth, and high critical current have raised considerable interest among researchers concerning its potential applications in thin film based devices.

Preliminary work investigating the electroless deposition of Lead films on a variety of substrates and MgB_2 films on copper established the suitability of this technique for preparing superconducting thin films [10]. However, these studies also found that the MgB_2 films prepared on Cu exhibited a superconducting fraction of only 0.1% and the film quality was strongly affected by the presence of oxygen and impurities during preparation of the precursor materials and the deposition process [11]. To address these limitations, we investigated the deposition of MgB_2 onto noble metals like silver and gold. Motivated by the observation that using substrate materials high on the electromotive force series (EMF) results in higher quality films, we extended our study to explore electroless deposition on silicon while controlling the oxidation potential of the electrolytic bath. Silicon, apart from being non-metallic, non-conductive in nature, it has many other advantages over gold and silver as cost, availability of the material. It is most widely used material in electronics industry and a junction between the study & application area of superconductors and semiconductors.

We conducted extensive physical characterization of these superconducting films. The crystallinity and microstructure of the samples were investigated using X-Ray diffraction, Raman spectrometry, and SEM imaging. The X-ray diffraction was done by a Rigaku rotating anode (Ru-2000) X-ray diffractometer, while the Raman used a Triax spectrometer and Ar^+-ion laser, and the SEM images were obtained on a Hitachi S-2400 system. We also conducted magnetic susceptibility measurements to probe the superconducting properties of these films using SQUID magnetometer (Quantum Design MPMS-5S) to obtain the DC magnetization and a Physical Property Measurement System (Quantum Design PPMS) capable of measuring both DC and AC magnetic susceptibility. X-ray diffraction and Raman spectroscopy confirmed the presence of

polycrystalline MgB_2 along with some impurities. All the films show a superconducting transition at 39 K, the value of bulk MgB_2 with superconducting volume fraction of 1 □2 %

CHAPTER 2 – LITREATURE REVIEW

2.1 – Superconductivity and its theory

Superconductivity was discovered by Kammerlingh Onnes in 1911. It is an element, inter-metallic alloy or compound that will conduct electricity without resistance below critical temperature. In many applications, Resistance is undesirable because it produces losses in energy flowing through the material. Once set in motion, electrical current will flow forever in a closed loop of superconducting material [12]

Electrical resistance in metals arises because electrons propagating through the solid are scattered due to deviations from perfect translational symmetry. These are produced either by impurities or defects or the phonons or lattice vibrations in a solid.

Inside a superconductor the behavior of electrons is quite different. The impurities and lattice are still there, but here the superconducting electrons travel through the material with no measurable loss in the current and energy [13]. Within a superconductor, electrons having opposite spin and momentum couple together to form **cooper pairs** which is held together by the lattice vibrations called phonons. This electron-phonon interaction gives rise to a highly correlated pair of conduction electrons which flow in a single coherent motion. Below T_c, the cooper pair are not scattered by defects in a crystal lattice and they flow without any dissipation [14]

The essential point is that below T_c the binding energy of a pair of electrons causes the opening of a gap in the energy spectrum at E_f (the Fermi energy), separating the pair states from the "normal" single electron states. The size of a Cooper pair is given by the coherence length which is typically 1000Å. The space occupied by one pair contains many other pairs, and there is

thus a complex interdependence of the occupancy of the pair states. There is then insufficient thermal energy to scatter the pairs, as reversing the direction of travel of one electron in the pair requires the destruction of the pair and many other pairs due to the nature of the many-electron BCS wave function. The pairs thus carry current unimpeded, at least for sufficiently small currents.

BCS theory has been successful in explanation of low T_c superconductors such as Nb3Ge (T_c = 23K). The central supposition of BCS theory is the idea that electrons at very low temperature behave like a super fluid and in the atomic lattice of a material, they couple together to form cooper pairs. The electrons are bound together by their interaction with the vibrations of the underlying lattice: one electron in the pair polarizes the lattice by attracting the nuclei towards it, leaving a region of excess positive charge (a potential well) into which a second electron is attracted - the positively charged nuclei thus mediate an attraction between the negatively charged electrons. Only electrons with energies close to E_f, strictly speaking, within $h\omega$, where ω is a characteristic phonon frequency, can be paired by this interaction, and so only a small fraction of the electrons become superconducting [15]

2.2 - Meissner Effect

The abrupt transition from the normal to superconducting state occurs at a boundary defined not only by the transition temperature (T_c) but also by magnetic field strength. There is a critical value of magnetic field, H_c, above which the superconductivity is destroyed [16, 17]. If a paramagnetic or diamagnetic material is placed in a magnetic field, then the magnetic lines of force penetrate through the material as shown in Figure 2.1(a). However when the same material is made superconducting by cooling to a low temperature below T_c then the magnetic lines of force are completely expelled from the interior of material, at least for small magnetic fields, as

shown in Figure 2.1(b). This effect is called **Meissner effect**. Based on Meissner effect, the superconducting materials are classified as Type 1 and Type 2 superconductors.

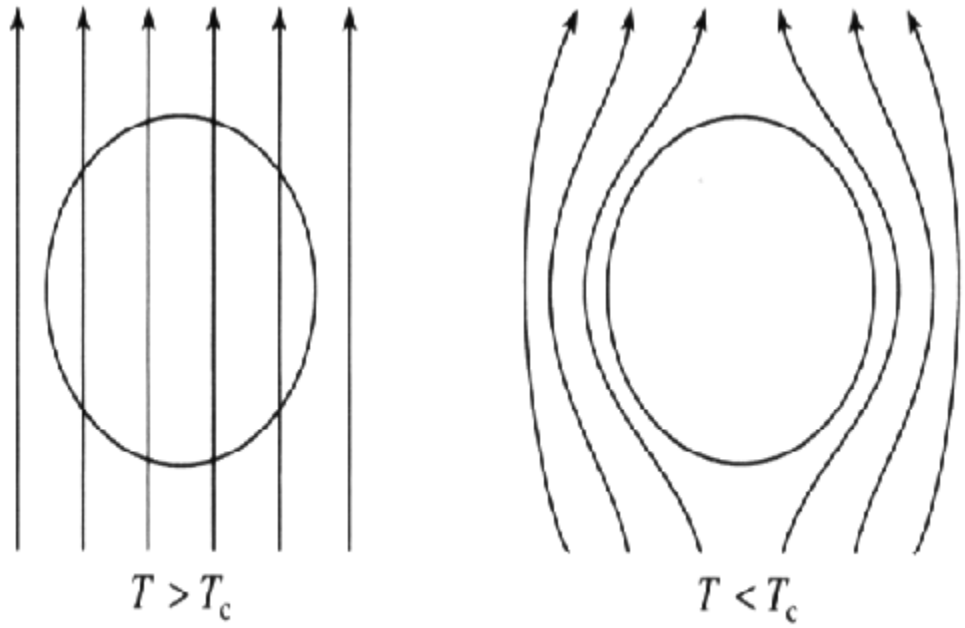

(A) (B)

Figure 2.1 The Meissner effect in superconductor

In **Type 1 superconductor** there is a sharp transition from superconducting state to normal state as shown in Figure 2.2 (a), with no magnetic flux ever penetrating the superconducting state [18]. This kind of behavior is shown by pure metals.

In **Type 2 superconductors** there are two values of critical field: the lower critical field, Hc1, and the upper critical field H_{c2}. For $H<H_{c1}$, the field is completely expelled from superconductor [19]. However for $H>H_{c1}$, the magnetic field penetrates the material slowly and continues to H_{c2}, beyond which the material transforms completely from superconducting state to

normal state. The state between H_{c1} and H_{c2} is called vortex or mixed state. Figure 2.2 (b) shows H-T phase diagram for conventional low T_c superconductors. At low fields, there is meissner effect and at high fields vortices enter the material from a vortex lattice. Superconductivity is completely destroyed H_{c2} for which the density of vertices is such that the normal cores fill the entire material. For low T_c superconductors, this behavior is exhibited, in general, by alloys and compounds. On the other hand all high T_c superconductors behave as Type 2 superconductors.

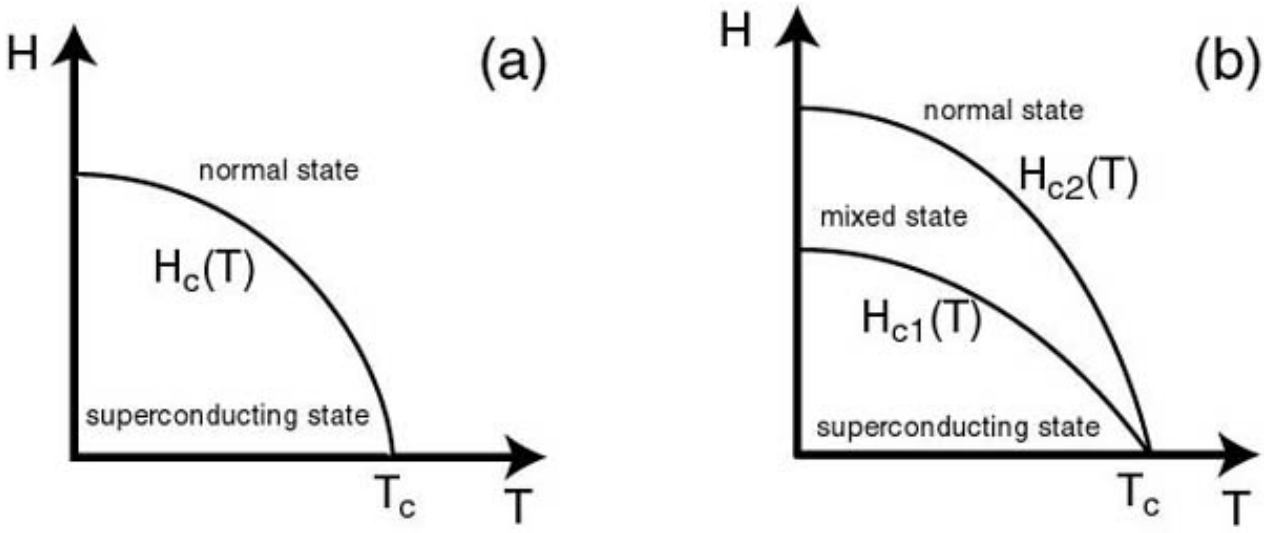

Figure 2.2 Types of superconductors

2.3 - High Temperature Superconductors

The high temperature superconductors represent a new class of materials which bear extraordinary superconducting and magnetic properties and great potential for wide-ranging technological applications. This class of materials not only show high temperature superconductivity but also shows properties that are different than classical superconductors.

They offer a great challenge to understanding the basic phenomenon that causes superconductivity in these materials and to developing the appropriate preparation. There has also been great progress in understanding the properties of materials developing different methods of preparation and realizing superconducting devices which use these superconductors [20].

The first of the high temperature superconductors to be identified was Ba doped La_2CuO_4 in 1986, which exhibited a transition temperature of T_c=30 K. This result was remarkable because the parent compound was anti ferromagnetic, insulating and because this transition temperature was much higher than what could be predicted by BCS theory [20]. Since then there have been many discoveries in the field of HTS classifying them into metallic low temperature superconductors, cuprate based, iron based and other high temperature superconductors.

The structure of high T_c superconductors is closely related to pervoskite structure discovered in 1986. The unit cell consists of two metal atoms A and B with three oxygen atoms with the general formula given as ABO_3 [20]. The ideal structure is as shown in the Figure 2.3. Atom A sitting at the body centered site is coordinated by 12 oxygen atoms. Atom B occupies the corner site and oxygen occupies the edge centered position.

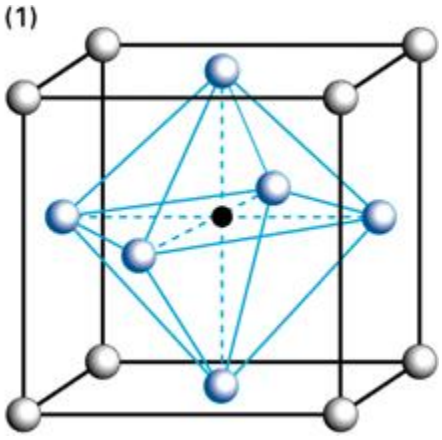

Figure 2.3 High temperature superconductors

High T_c superconductors are prepared in form of bulk, thick films, thin films, single crystals, tapes and wires. Strict control of stoichiometry of composition is very much required for preparing high T_c superconductors with desirable characteristics. Even a small change in oxygen content or cation doping level can transform the material from a superconductor to a low carrier density metal or even to insulator.

For thin films different techniques such as sputtering, evaporation, molecular beam epitaxy, laser ablation, chemical vapor deposition and so forth have been used for thin film high T_c superconductors. Most of these techniques work in vacuum environment and the oxygen partial pressure near the substrate is controlled to obtain superconducting thin film. This can be done during film deposition or post deposition annealing. The substrate temperature during deposition is a crucial parameter that determines microstructural details such as texture and degree of epitaxy. It is desirable to develop low temperature process to maintain good quality films and prevent substrate film interaction.

2.4 Magnesium Diboride and its Properties

The discovery of its superconducting nature with T_c 39 K [22] was announced by Nagametsu and his co-workers in Journal Nature 2001. The critical temperature is the highest among the superconducting transition temperatures of all metallic compounds, but still smaller in comparison with that of some other high T_c superconductors, such as the cuprate superconductors. MgB_2 does not require the very low temperatures of conventional superconductors, so it would be used to fabricate devices that operate in liquid helium, liquid hydrogen, or cryocoolers. As a consequence of large coherence length, this compound has weak free grain boundaries, and therefore, high transport current densities of order of 10^6 A/cm^2 and high upper critical magnetic field in the temperature range from 4.2 K to 25 K in bulk sample.

Another important reason to count MgB_2 as a promising candidate for industrial application is because it's low cost and it is abundantly available. Practical long-length multifilament conductors can be made more inexpensively than niobium-based low temperature superconductors and sterling silver-clad low temperature superconductors. The density of MgB_2 is comparable to aluminum, leading to its uses in lightweight applications as well.

MgB_2 has a simple hexagonal crystal structure with P6/mm symmetry in which graphite like honeycomb layer of boron atoms is stacked in between two hexagonal layers of magnesium atoms. This structure is very similar to that of graphite where each carbon atom – which has four valence electrons – is bonded to three others and occupies all planar bonding states (the sigma bands) [23]. The remaining electron moves in orbitals above and below the plane to form pi bands. Boron atoms have fewer valence electrons than carbon so not all of the sigma bands are occupied. This means that lattice vibrations in the planes are much larger, which results in the formation of strong electron pairs [24]. Even though superconductivity in MgB2 is much lower than high temperature cuprates it is important because of its superiority over high T_c materials. Firstly it is made up of light and cheap elements abundantly in nature. Secondly, unlike cuprates MgB_2 doesn't have high contact resistance between grain boundaries eliminating weak link problem that has plagued wide spread commercialization of the cuprates. Further, the conduction electron density and normal state conductivity are one to two orders of magnitude higher for MgB_2 than for the cuprates in the present day wires and thin films [25]. These features make MgB_2 attractive for many applications.

We now discuss some of the experiments on MgB_2 thin films in restricted geometry. Thin films have a wide range of applications in electronic industry e.g. digital convertors, transmitters and receivers. Thin films are also useful for their power storage, transmission and consumption

of extremely low power. There has been a significant amount of work done on developing MgB_2 wires and films that could be used for commercial applications. Hot isostatic pressing of wires made of magnesium diboride has shown that the critical current for these wires are significantly higher than Nb based superconductors.

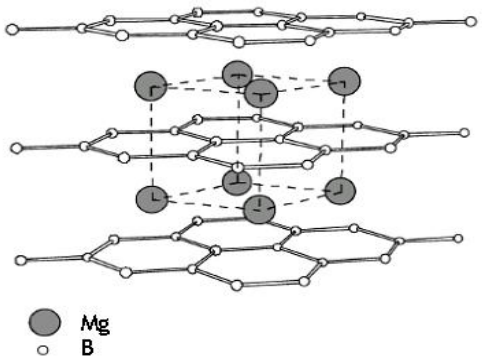

Figure 2.4 The crystal structure of Magnesium Diboride

Filaments made from MgB_2 could significantly reduce the costs for applications using superconducting wires such as magnetic resonance imaging and electrical generators. At present, a large number of groups around the world are engaged in the fabrication of wires and the preparation of high quality thin films for possible device applications. However, fabricating MgB_2 films is complicated because of large differences in vapor pressure between B and Mg and because Mg oxidizes easily. These problems do not arise in the electroless deposition process. MgB_2 may also prove to be useful in developing devices for electronic applications as well. Thin films of MgB_2 may have applications in thin film geometries based superconducting devices such as Josephson junctions and superconducting quantum interference devices (SQUIDs).

Many workers have been successful in growing MgB_2 films using different techniques, such as pulsed laser deposition, molecular beam epitaxy, dc magnetron sputtering, hybrid physical–chemical vapor deposition, co-deposition and electrophoresis. These methods consist of

two-step growth processes. The first step is deposition of Mg–B or B precursor films and the second step is high-temperature annealing in Mg vapor. The high-temperature process involved in the above methods, however, hinders the fabrication of multilayer and high-quality Josephson tunnel junctions. To fabricate Josephson tunnel junctions with MgB_2 films, a low-temperature method of depositing as-grown MgB_2 thin films needs to be developed.

2.5 Electroless Plating

The technique of using a redox reaction to deposit metal on surface without use of electric current is termed as **Electroless plating** The chemical deposition of a metal from an aqueous solution of a salt of said metal has an electrochemical mechanism of involving both oxidation and reduction reactions involving the transfer of electrons between reacting chemical species [8]. The oxidation of a substance is characterized by the loss of electrons, while reduction is characterized by a gain of electrons. Further, oxidation describes an anodic process, whereas reduction indicates a cathodic action. For example when magnesium metal is immersed in copper sulphate solution, the magnesium metal atoms dissolve and are spontaneously replaced by copper atoms.

Oxidation	$Mg \longrightarrow Mg^{2+}(aq) + 2e$	$E^o = +2.36$ V	(1)
Reduction	$Cu^{2+}(aq) + 2e \longrightarrow Cu(s)$	$E^o = +0.34$ V	(2)
Overall Equation	$Mg(s) + Cu^{2+}(aq) \rightarrow Mg^{2+}(aq) + Cu(s)$	$E^o = +2.70$ V	(3)

In order to continuously build thick deposits by chemical means without consuming the substrate, it is essential than a sustainable oxidation reaction be employed as an alternative to the dissolution of the substrate. The deposition reaction must occur initially and exclusively on the substrate and subsequently continue to deposit on the initial deposit. The redox potential for this

chemical process is usually more positive than that for a metal being deposited by immersion. In general, electroless plating is characterized by the selective reduction of metal ions only at the surface of a catalytic substrate immersed into an aqueous solution of said metal ions, with continued deposition on the substrate through catalytic action of the deposit itself. Since the deposit catalyzes the reduction reaction, the term autocatalytic is also used to describe the plating process. This process offers distinct advantages when plating irregular shaped objects, holes, recesses, internal surfaces, valves or threaded parts.

Electroless deposition of metals can be explained as the sum of the cathodic reduction of the metal combined with the anodic oxidation of the reducing agent, both on the catalytic surface. In addition, there might be also some interference effects between the reactions. Therefore, the complete reaction is a result of a combination of two different partial reactions. Those two partial reactions, however, occur at one electrode, the same metal/solution interface. For example the chemical deposition of cobalt metal by hypophosphite requires partial reactions meeting both oxidation and reduction reactions without changing mass of substrate.

Reduction $Co^{2+} + 2e- \longrightarrow Co^{o}$ (4)

Oxidation $H_2PO_{2-} + H_2O \longrightarrow H_2PO_{3-} + 2H^{+} + 2e-$ (5)

Overall Reaction $Co^{2+} + H_2PO_{2-} + H_2O \longrightarrow Co^{o} + H_2PO_{3-} + 2H^{+}$ (6)

All of these postulations were made on a base of the Wagner-Traud mixed potential theory of corrosion processes [26]. According to this theory, the rate of a faradaic process is independent of other faradaic processes occurring simultaneously at the electrode and thus depends only on the electrode potential. Hence the polarization curves for the independent anodic and cathodic processes may be added to predict the overall rates and potentials which

exist when more than one reaction occurs simultaneously at an electrode. According to the Wagner and Traud theory electroless metal plating processes have been identified as mixed potential systems**,** and it has been suggested that the electroless plating mechanisms can be predicted from the polarization curves for the partial processes. Such polarization curves can be obtained by one or more of the following methods:

1. By applying the steady-state galvanostatic or potentiostatic pulse method to each partial reaction separately;
2. By applying potential scanning techniques to a rotating disk electrode;
3. By measuring the plating rate from the substrate weight-gain as a function of the concentration of the reductant or the oxidant.

The plating rate is then plotted against the mixed potential to obtain the Tafel parameter. Application of the mixed potential theory has led to a technique by which electroless plating processes may be classified according to their overall mechanisms.

2.5.1 Thermodynamic Analysis of Electroless Plating

The autocatalytic metal reduction reactions are classified as redox reactions with the metal as a final product. Such reactions may take place both in aqueous and non aqueous media. Metals that are thermodynamically stable in water are candidates for autocatalytic reduction in aqueous media. Such metals are Fe, Cd, Tl, Co, Ni, Sn, Pb, Bi, Re, In, Cu, Hg, Pd, Pt and Au [26]. However, reactions that are possible from thermodynamics considerations are retarded due to the reaction's kinetics and the overall deposition rate is very low. Moreover, the product of the autocatalytic metal reduction does not necessarily from continuous metal layer. It may be high porous deposit or metal powder. The autocatalytic metal reduction reactions have top chemical nature, *i.e.*, they occur at the interface between the product and the reaction media.

Consequently, the reaction has many stages and there are many parameters that govern the overall reaction kinetics. Among those parameters are the following:

a) Transport phenomena of reactive species in the liquid

b) Transport phenomena of the reactive species at the solid/liquid interface

c) Transport phenomena of adsorbed species on the interface;

d) The nucleation kinetics

e) The kinetics of the electrochemical and chemical reactions that take place at the liquid and solid/liquid interface

2.5.2 Advantages of Electroless Plating

a) Excellent uniformity of coating thickness, demonstrating 100% Throwing Power [28]

b) Bulk processing capability

c) Ability to produce unique catalytic coatings

d) Ability to coat non-conductive materials such as ceramics and plastics.

e) No need to use electric power and electrical contacts are eliminated

f) Homogenous chemical, mechanical and magnetic properties.

g) It can be used to uniformly coat irregular shaped objects.

2.5.3 Applications of Electroless Plating

1. Plating on Plastics: The plated plastic parts having many potential uses. In consumer products plating has been used primarily for decorative purposes. It has many functional advantages in the plumbing and marine industries as electroless plated parts are far more corrosion resistant than electroplated parts.

2. Solderability: Electroless nickel has been widely used in soldering aluminum parts. It is similarly effective for steel

3. Electronics: The application is for plating through holes in printed circuit boards. Plated holes are used to provide either a conducting path for the two sides of the board or wicking path for solder during installation.

4. Automotive: Shock Absorbers, heat sinks, gears, cylinders, brake pistons etc.

5. Aviation & Aerospace: Satellite and rocket components, rams pistons, valve components etc.

6. Oil & Gas: Valve components, such as Balls, Gates, Plugs etc. And other components such as pumps, pipe fittings, packers, barrels etc.

OBJECTIVE

The primary objective is to develop a novel electroless plating process for the synthesis of thin films of superconducting magnesium diboride on a range of insulating, conducting and semiconducting substrates. The secondary objective is to characterize these films using different analytical techniques including X ray diffraction, magnetic susceptibility, energy dispersive X-ray analysis and Raman spectroscopy to ascertain the reproducibility and durable superconducting properties of these films. In order to prepare compound superconducting films using novel electroless plating technique, it will be necessary to obtain the relevant thermodynamic data and determine the rate controlling mechanism for this process. These studies will clarify the role of oxidation potential during the deposition process.

2.6 Plating Variables

The chemical and physical properties of electroless plating depend on its composition, which, in turn, depends on the formulation and operating conditions of the plating bath. The constituents of the solution are:

- Source of metallic ions
- A reducing agent
- Suitable complexing agent
- Stabilizer/Inhibitors
- Energy

Every plating process requires and benefits from process control. It is vital to achieve the desired properties. Most commonly desired properties include corrosion resistance, hardness and wear resistance. The chemistry, operating parameters, surface preparation and equipment considerations are the primary variables that influence deposition rate, coverage, adhesion, smoothness, uniformity and brightness [29].

The three primary areas include the chemical balance, the interaction of rate and loading effects and the influence of the process equipment on the final quality.

2.6.1 Chemistry and chemical balance

The key to a successful plating system is proper replenishment. Neglecting replenishment schedules or maintenance of solution levels can cause non-uniform deposits, premature bath decomposition, slow deposition rates, poor adhesions, poor brightness, pitting or roughness [29]. Usually, the effects of poor bath control are seen immediately after the parts have been plated. With a variety of chemical materials comprising these systems, an imbalance will likely cause some negative result.

2.6.2 Stabilizers

Stabilizers are important in regulating the plating rate while also preventing the solution from spontaneously decomposing.

2.6.3 Magnesium and Boron controls

As the metal ions decreases, the rate of deposition decreases. A decreasing Mg and B concentration affects the coverage, brightness and uniformity of the deposit through a reduction of the plating rate or initiation of plate. In order to maintain these properties at an optimum level, small frequent additions should be made. In addition to stabilizer effects than can result, large chemistry replenishments tend to shock the solution, possibly resulting in salt precipitation, deposit porosity and roughness, especially in aged baths.

2.6.4 Hypophosphite

The reducing agent is consumed both productively and non-productively during plating. The reducing agent influences plating efficiency. During plating, the sodium hypophosphite reducing agent, “the chemical rectifier”, is consumed in a given ratio to the metals in plating. The reducing agent is also consumed non-productively through hydrolysis, which occurs, when solution is kept at the operating temperature and not used to plate. To optimize, the hypophosphite efficiency, it is important to heat up and cool down the solution quickly while maintaining a constant process load in the tank when solution is heated.

2.6.5 Contamination

The concentration of trace metals and other contaminants within the plating solution will affect deposit quality and appearance. Some metals may also tend to act as stabilizers and/or catalytic poisons that inhibit plating. Elements that act as stabilizers include sulfur, cadmium,

bismuth, antimony, mercury, lead, zinc and iron. Source of organic contamination include masking agents, oils, plasticizers.

2.6.6 Operating pH

The solution's operating pH is an important parameter because it affects the plating rate and amount of phosphorous co-deposited. Higher pH values favor lower phosphorus contents in the deposit while increasing the plating rate. Higher pH values, within the range for the particular system used, can lead to precipitation of metal hydroxides or orthophosphates. The precipitation normally causes porosity, which affects corrosion resistance. The pH is easily checked electrometrically or with pH papers.

2.6.7 Operating Temperature

The temperature of plating solution is one of the most important factors affecting deposition. It is important to have the proper heating system to avoid localized overheating, which can result in bath decomposition or deposit roughness. It also has an influence on deposit smoothness, coverage and adhesion.

CHAPTER 3 - EXPERIMENTAL PROCEDURE

3.1 Surface Preparation

An important characteristic of plating metals is the strength of the bond that can develop between the base metal and coating. Metal to metal bonds with high adhesion values require thorough surface preparation – removing from base metal surface foreign contaminants and eliminating mechanically distorted surface layers to present a clean healthy surface structure. The surface contamination can be extrinsic, comprised of organic debris and mineral dust from the environment or can also be intrinsic, an example being a native oxide layer [30]. Cleaning methods needs to be carefully selected and designed to minimize substrate damage. An improper treatment can affect and thus increase the porosity of metal substrate, creating more passive spots that will not initiate electroless plating.

3.1.1 Surface Preparation on Copper / Silver / Gold

3.1.1.1 Alkaline Soak Clean

The first step in pre-treatment was carried out using DS Ronaclean GP 300 LF, a low foaming high detergency alkaline soak cleaner. It is designed for primary cleaning of metals with or without use of organic solvent degreasing. A copper metal strip was immersed in alkaline solution for 2 – 3 minutes, when the solution was maintained at a temperature of 70 deg C. The solute concentration was 40-55 g/l and it was diluted using de-ionized distilled water.

3.1.1.2 Water Rinse

Through the entire pre-treatment process, the metal plate was rinsed in de-ionized water in between steps in order to remove alkaline salt residues and unwanted impurities settled on the surface. The de-ionized water was obtained from U.S Filter Pure lab having resistivity of 18

M/cm for all rinsing operations. The de-ionized water rinsing is essential after every step to prepare the surface for next efficient cleaning procedure.

3.1.1.3 Electrolytic Clean

Electro cleaning is the normal way to prepare parts for electroless plating. In this case we used anodic electro cleaning for final cleaning. The metal surface is actually being dissolved as well as cleaned. This action removes metallic smuts and prevents deposition of non-adherent metallic particles. At the interface of metal and solution oxygen is liberated which helps removing soil.

The solution used was alkaline salt of Ronaclean GP 300 LF at concentration of 45-60 g/l. It was heated to a temperature of 65-85 deg C for 2-3 minutes with copper connected to anode and graphite to cathode. A direct electric current supply of 5V was passed through the solution.

3.1.1.4 Acid Clean

It is a process where a solution of a mineral acid, organic acid, or acid salt in a combination of wetting agent and detergent is used to remove oxide, shop soil, oil, grease and other contaminants from the metal surfaces with or without application of heat. In our experiment we soaked the copper foil in 2-5 % dilute sulphuric acid for 1-2 minutes at room temperature to remove the alkaline residues left behind after alkaline soak clean and electro clean.

3.1.2 Surface Preparation on Silicon

The main difference between metallic and non metallic surfaces resides in the nature of bond between substrate and coating. The adhering to metal is atomic in nature but to non metallic is mechanical in nature. It is necessary to attain a right topography on silicon by

chemical and mechanical treatment. Their non catalytic nature requires them to undergo activation treatments.

3.1.2.1 Etching

The silicon as described in earlier text requires a good mechanical treatment before the sensitization and activation steps. The substrate is etched using by 2-20 % dilute hydrofluoric acid with 18g/l of Aluminum fluoride dissolved in HF solution for 5-10 mins at room temperature.

3.1.2.2 De-Ionized Water Rinse

The etching is followed by water rinse to remove the fluoride residues left behind on the non-metallic substrate. The water was obtained from U.S Filter Purelab Plus deionization unit having resistivity of 18 M/ cm for rinsing operations. The water rinse is performed on substrate after each step of the cleaning process.

3.1.2.3 Sensitizing

This is a process of forming catalytic nuclei for electroless plating thereon, before immersing in electroless plating bath. Sensitizing for silicon is accomplished by immersing parts in a 50g/l of acid stannous chloride solution at room temperature for 5 minutes.

3.2.1 Surface Activation on Copper / Silver / Gold

In a process of electroless plating of magnesium Diboride onto a substrate of copper an aqueous solution of magnesium Diboride is used as an activator on to the substrate prior to the plating. The activation bath contains 1% MgB_2 plating solution and the copper metal strip is dipped in the solution for 30-40 seconds at a temperature of 50-60 deg C with using copper as cathode and cleaned stainless steel as anode. A steady electric current of 5V from a DC source is

passed through the weak electrochemical bath. The metal strip needs to be rinsed off before final electroless plating procedure.

3.2.2 Surface Activation on Silicon

To make the surface active the substrate is treated with 0.1 – 0.5g/l of palladium chloride with 1-3 g/l of hydrochloric acid at room temperature for 5-10 minutes. After activation the parts should be ready for electroless plating with hypophosphite electroless MgB_2 solutions. It must be remembered that final adherence of electroless deposit will not only depend on pretreatment, but also on the characteristics of the plating process

3.3 Electroless Deposition

The cleaned and pre-treated substrate is used for electroless plating technique. For our experiments we carried out two different plating bath conditions. In case of silver and gold substrate we have made use of acidic medium based electroless plating bath solution and for copper and silicon plates we use an alkaline based electroless bath solution. The parameter details and bath conditions for each of them as explained below

3.3.1 Electroless plating for Silver and Gold (Acidic Medium)

The electroless plating of MgB_2 on silver and gold required an acidic bath with a high redox potential. The plating bath contained MgB_2 powder, a reducing agent (Sodium hypophosphite), a complexing agent (Sodium Succinate), a buffer (Sodium acetate) and Dimethyl Sulphoxide (80 ml/L) to prevent oxidation. The operating temperature of the bath was held between 70-75˚C with the pH maintained at 6±0.5. The plating process was carried out in a dry argon atmosphere.

3.3.2 Electroless plating for Silicon and Copper (Alkaline Medium)

We used an alkaline bath with a low redox potential for the electroless deposition of MgB_2 on silicon. This plating bath was composed of MgB_2 powder, Sodium citrate, and Sodium hypophosphite. Sodium citrate was used as the complexing agent, sodium hypophosphite as the reducing agent. We also added ammonium hydroxide (NH_4OH) to adjust the pH to 12±0.5, with the temperature held at 73±3^{o}C. The molar concentration of MgB_2 in the plating bath was kept at 0.2 M, which was experimentally determined to yield the best results for this system.

Chemical Property	**Value**
MgB_2 Salt	0.6 g
Sodium Hypophosphite	1.04 g
Sodium Succinate	0.5 g
Dimethyl Sulfoxide	4 ml
Sodium Acetate	1.20 g
Temperature	70-80 deg C
pH	6.5 – 7.5
Time	120 min

Table 3.1 Composition of acidic plating bath

Chemical Property	Value
MgB_2 Salt	0.6 g
Sodium Hypophosphite	1.25 g
Sodium Citrate	3.0 g
Ammonium Hydroxide	2 ml
Temperature	70-80 deg C
pH	12 +
Time	120 min

Table 3.2 Composition of alkaline plating bath

The chemical reduction of Magnesium diboride on the catalytic surface can be represented by following reactions.

Ionization of water at surface

$2H_20 \longrightarrow 2H^+ + 2OH^-$

Coordination of hydroxyl ions to solvate magnesium diboride

$Mg(H_20)_x^{+2} + 2OH- \longrightarrow Mg(OH)_2 + 2H_2O$

$Mg(OH)_2 + H_2PO_{2-} \longrightarrow B(OH)_3 + H_2PO_{2-} \longrightarrow Mg(OH)_{ads}\ B(OH)_{ads} + H_2PO_3^- + H$

$Mg(OH)_{ads} + B(OH)_{ads} + H_2PO_2^- \longrightarrow MgB^\circ + H_2PO_3^- + H$

3.4 Annealing of as-deposited MgB_2 film

The as-deposited MgB_2 were annealed in a sealed tube furnace under presence of nitrogen at 250 deg C for 2 hours to convert the film into polycrystalline superconducting phase. The annealed films were then ready for analysis of material properties.

3.5 Characterization of deposited sample

3.5.1 Surface Morphology

The annealed and crystallized films of magnesium Diboride were surface analyzed using high resolution scanning electron microscope Hitachi S-2400. The analysis was performed on all substrates.

3.5.2 Compositional Analysis

X-ray diffraction analysis (XRD) was performed using Rigaku Ru-2000 Rotating Anode Diffractometer. The X-ray diffraction technique brings out detailed information about chemical composition and crystallographic structure of MgB_2 superconductor. All X-ray examinations were carried out using Cu Kα radiation having wavelength 0.154 nm with 2θ range from 0˚ to 80˚ was used.

3.5.3 Temperature Dependent Magnetization Measurements

The magnetic susceptibility measurements i.e. magnetization as a function of temperature and magnetic field was measured using SQUID magnetometer (Quantum Design MPMS-5S) that has DC magnetic susceptibility to 10^{-8} and a Physical Property Measurement System (Quantum Design PPMS) capable of measuring both DC and AC magnetic susceptibility. All samples were cooled from well above the critical temperature at zero magnetic field and temperature dependant magnetization under different applied fields.

CHAPTER 4 - RESULTS & DISCUSSIONS

4.1 Compositional Analysis

The XRD analysis patterns of the annealed films of silver, copper and silicon are shown in Figure 4.1. The pattern on silver exhibited polycrystalline MgB_2 peaks along with some impurity phases of MgB_4, MgB_6, and MgB_{12}.

The XRD diffraction pattern of all these thin films are indexed using XRD PDF# 38-1369 (MgB_2), PDF# 15-0299 (MgB_4), PDF# 15-0298 (MgB_6), PDF# 08-0263 (MgB_{12}), PDF#30-0794 (MgO). The pattern also shows presence of underlying substrate of silver. In order to establish whether these impurity phases were present before deposition process the precursor salt was analyzed using X-ray diffraction. The analysis confirmed that the impurities were accumulated during the electroless plating technique, hence providing a significant opportunity for improving the film quality possibly by adjusting the processing conditions.

The XRD pattern on copper (not shown) and silicon shown in Figure 4.1 has MgB_2 peaks at 2θ reflection angle of 42.40˚ and 33.48˚ indicating the formation of crystalline MgB_2 phase with hexagonal P6/mm symmetry. The experimental procedure on these substrates was based on an alkaline medium plating process to that of silver in acidic medium. All fabricated films on different substrates are polycrystalline in nature, which we also confirmed from our SEM analysis, showing different grains with different orientations.

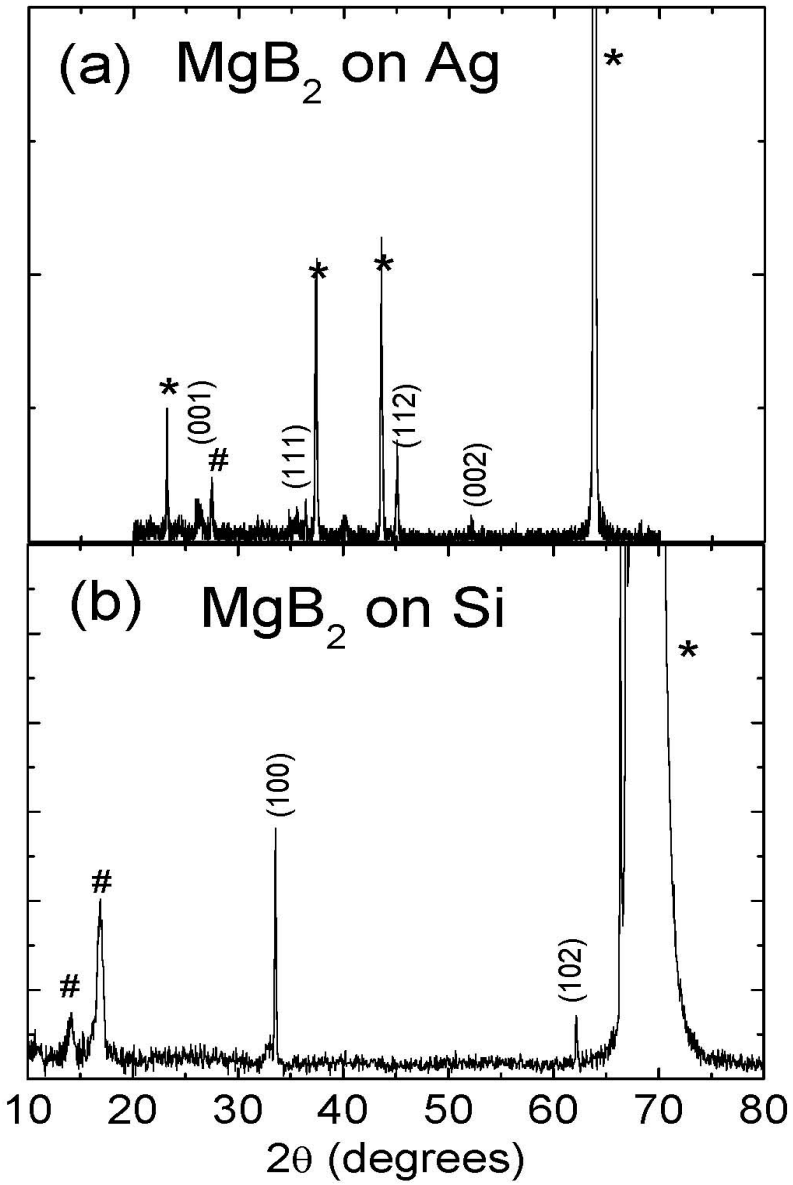

Figure 4.1 XRD pattern of the as-deposited MgB_2 film on (a) Ag, and (b) Si substrates. The MgB_2 peaks are indexed, with substrate peaks labeled with an asterisk (*) and the impurity peaks are labeled by the number sign (#).

4.2 Surface Morphology

4.2.1 Silicon Substrate

Post annealed film is as shown in Figure 4.2. The image shows a homogeneous uniform film with a few cracks. The film appears to have good connectivity except in a few sections, giving us the opportunity to improvise on continuous film which bodes well for applications involving electroless plated MgB_2. The film thickness for silicon was found to be 13.5 μm on a consistent basis. The film crack length was around 80-140 μm. These are not good for any application of point of view. These cracks may be arising during the annealing i.e. growth of the sample. The thermal expansion of the MgB_2 (approx) 2.6×10^{-6} / deg K and silicon (approx) 1.09×10^{-5}/ deg K causes the film to crack over the plate. In order to prevent this, thermal expansion studies requires to be analyzed in depth and different techniques of annealing needs to be employed.

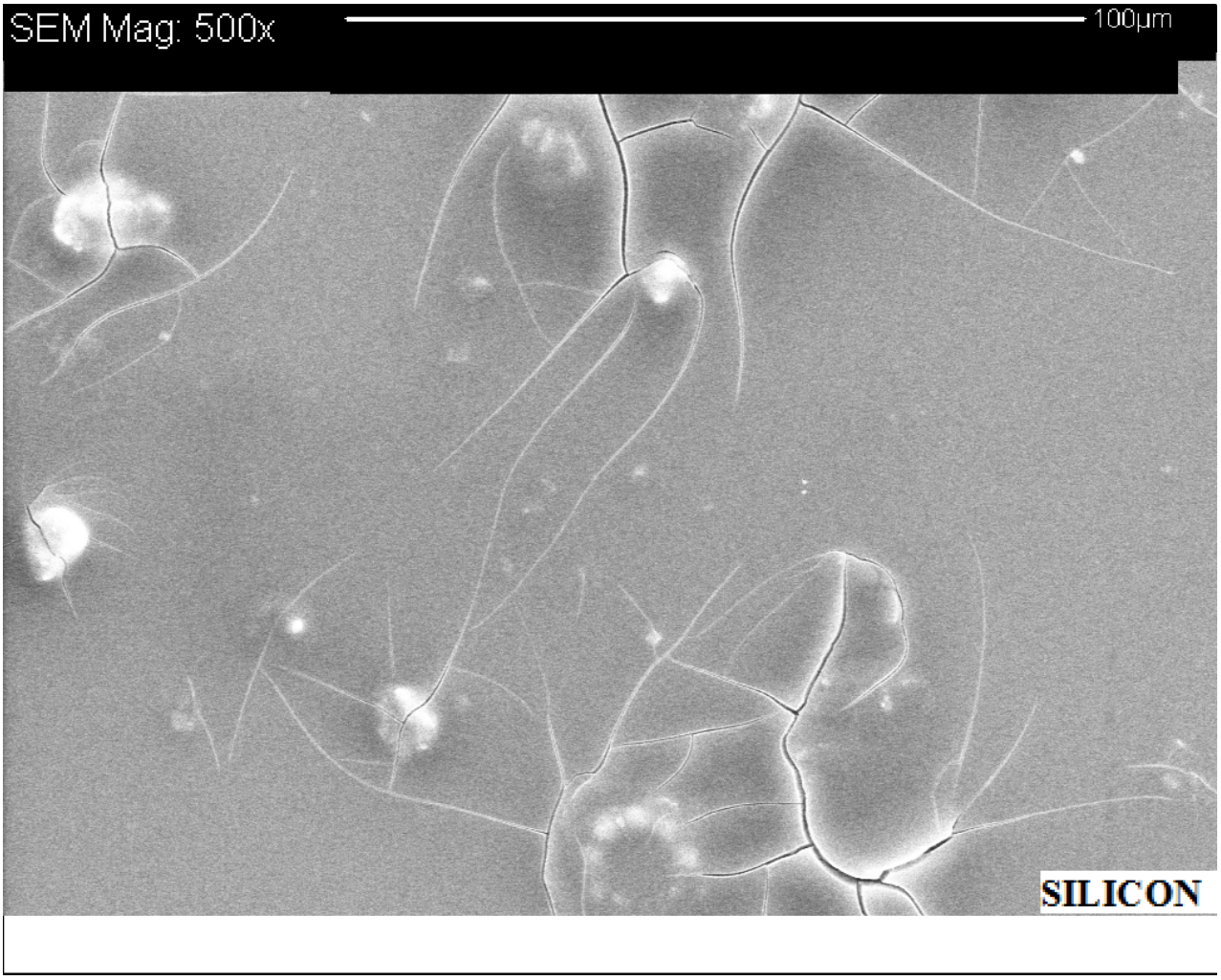

Figure 4.2 SEM image of MgB_2 film deposited on silicon substrate using electroless plating

The Figure 4.3 below is another representation on MgB_2 on silicon substrate. The crystals are observed in form of minute grain like structures that are closely bounded with a few areas where the silicon substrate is seen. These sites exhibit sections with no adhesion of magnesium diboride. Silicon being non-metallic in nature possesses poor activation sites compared to metallic substrates that are atomic in nature. This irregularity and poor adhesion may be due to poor catalytic sites generation during pretreatment preventing the nucleation of chemical. Hence a better chemical and mechanical treatment is required for a more continuous uniform deposit.

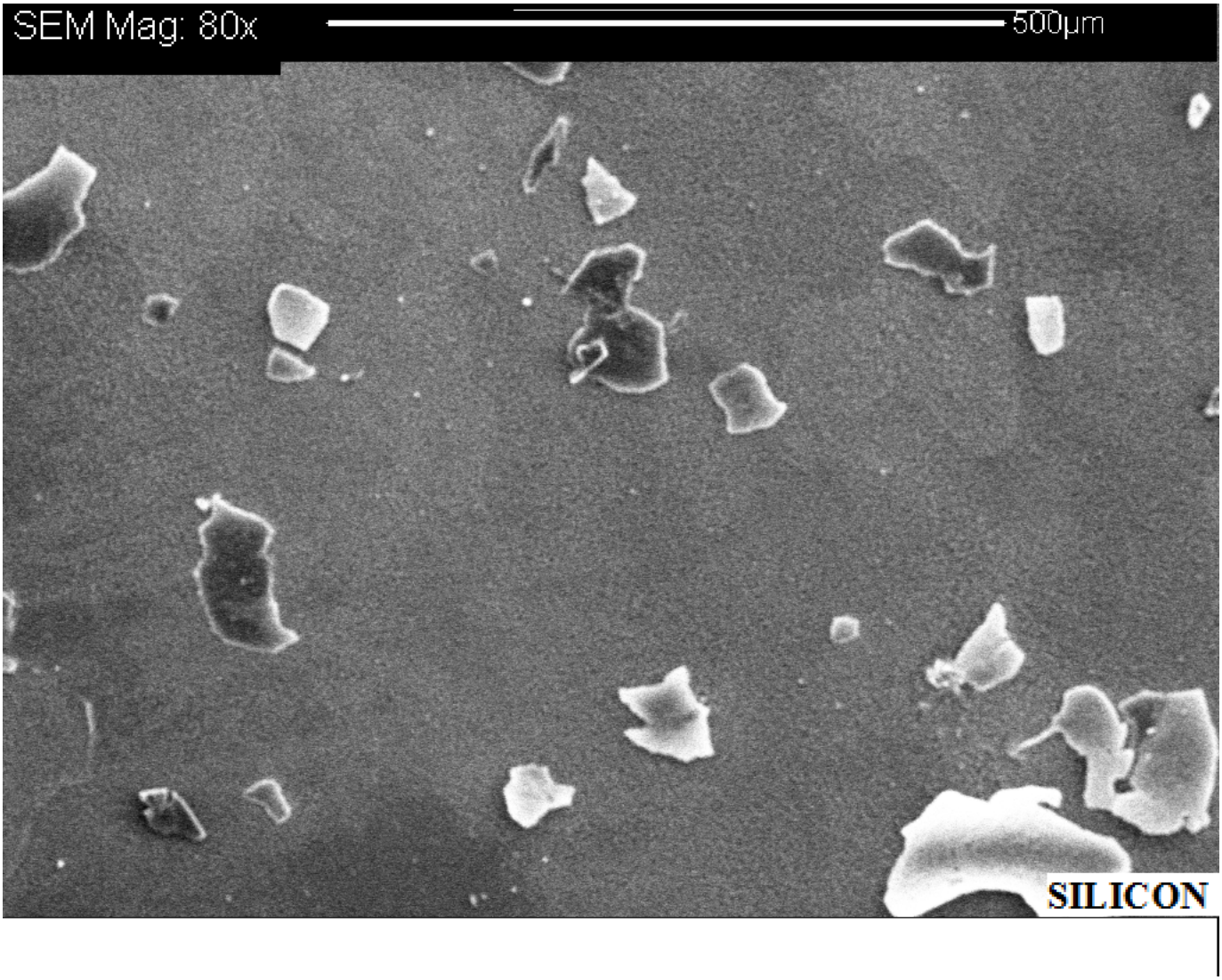

Figure 4.3: SEM image of MgB_2 film deposited on silicon substrate using electroless plating

4.2.2 Copper

Figure 4.4 shows synthesis of MgB_2 on copper substrate. The image suggests a uniform with good connectivity. It exhibits a difference in coloration throughout the surface that may be due to presence of oxides and impurities. The film is made of different crystallites of varying sizes and orientation due to its polycrystalline nature. The variation in crystallographic directions can be random or directed due to films growth and processing conditions. The polycrystalline MgB_2 is made of many monocrystalline modules. Polycrystalline compounds are less efficient but easier to produce and inexpensive.

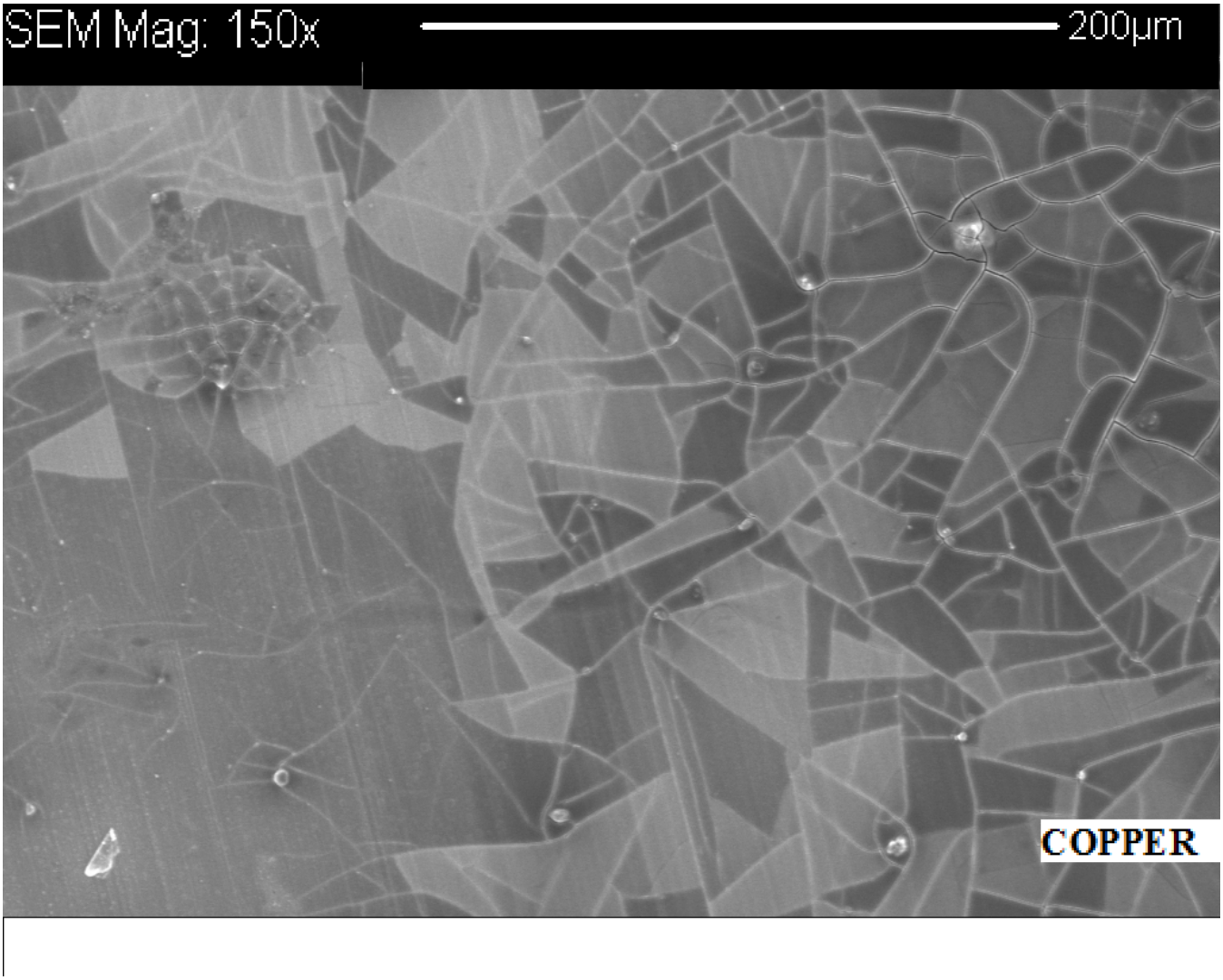

Figure 4.4 SEM image of MgB_2 film deposited on copper substrate using electroless plating

These films are polycrystalline and in our SEM images reflect it showing different grains across the films. The grains for MgB_2 on Ag, Cu are randomly sized, while MgB2 film is highly textured along (100) direction.

4.2.3 Thin film Dimensional Thickness

A microscopically thin layer of material is deposited on metallic and non metallic substrates as shown below in Figure 4.5. The coating thickness was 13.5 μm on silicon and 1μm on silver.

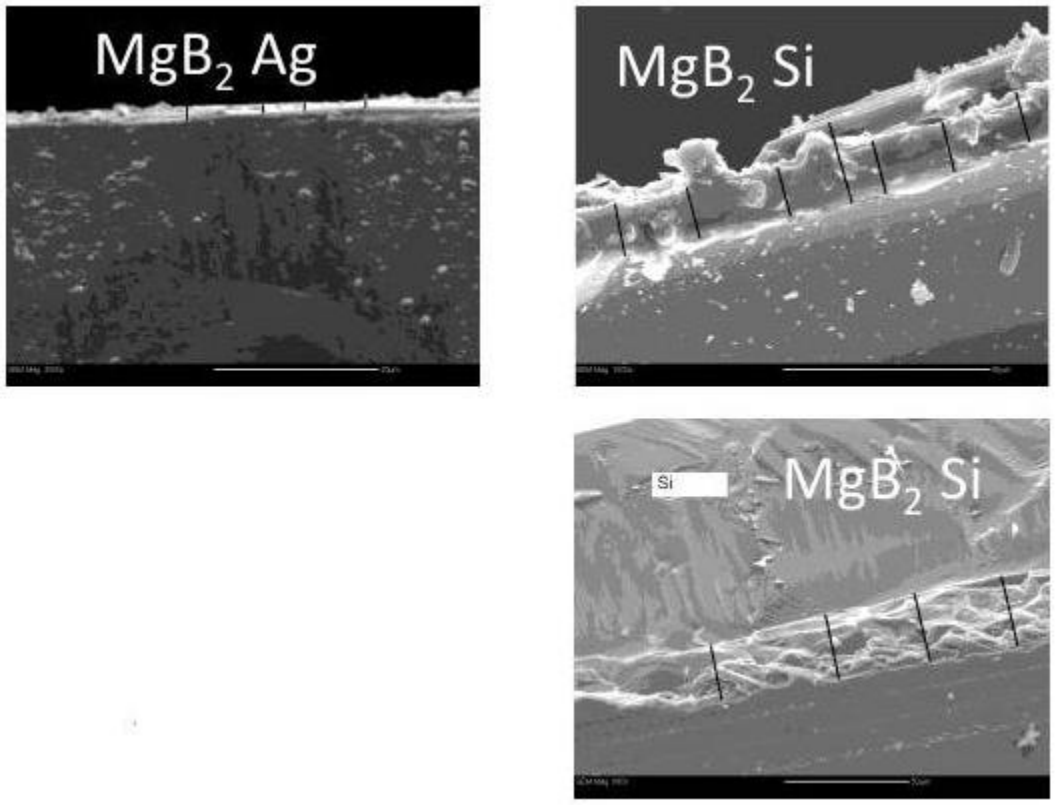

Figure 4.5 Thickness of MgB_2 film on silicon and silver

4.3 Temperature Dependent Magnetization Measurements

4.3.1 Gold and Silver

Magnetization measurements were performed with SQUID magnetometer and a Physical Property Measurement System to determine the superconducting properties of the deposited samples. The temperature dependent magnetic susceptibility for polycrystalline MgB_2 thin films on Au and Ag is as shown in Figure 4.5. The figure shows the magnetic susceptibility ($\chi = M/H$, where M is magnetization and H is magnetic field) as a function of temperature under conditions of zero field cooling and field cooling at 200 Oe. The susceptibility is plotted in dimensionless unit as a fraction of the susceptibility for a perfect diamagnet, appropriate for a superconducting fraction of 100%. The susceptibility has been corrected for background diamagnetic contribution from substrates by shifting high temperature susceptibility to zero. The measured magnetization with no background correction for the MgB_2 film on Ag is shown in Figure 8. It can be seen that the magnitude of raw signal is on the order of 10^{-6} emu. The existence of superconducting phase is confirmed by measuring Meissner effect on cooling in magnetic field. The onset of well defined Meissner effect was observed at 40 K. From the diamagnetic signature we estimate the superconducting transition temperature of 40 K to be consistent with the superconducting transition temperature for bulk MgB_2. The transition is rounded for sample prepared on gold, whereas the sample on silver shows a clear and sharp drop around 38 K. This indicates that the film prepared on gold may have structural defects or a more inhomogeneous composition compared to the film on silver, thus exhibiting a broadening effect. Using diamagnetic signal as a measure of superconducting fraction we determined the superconducting fraction for gold was 1% and that of silver was found to be 2%.

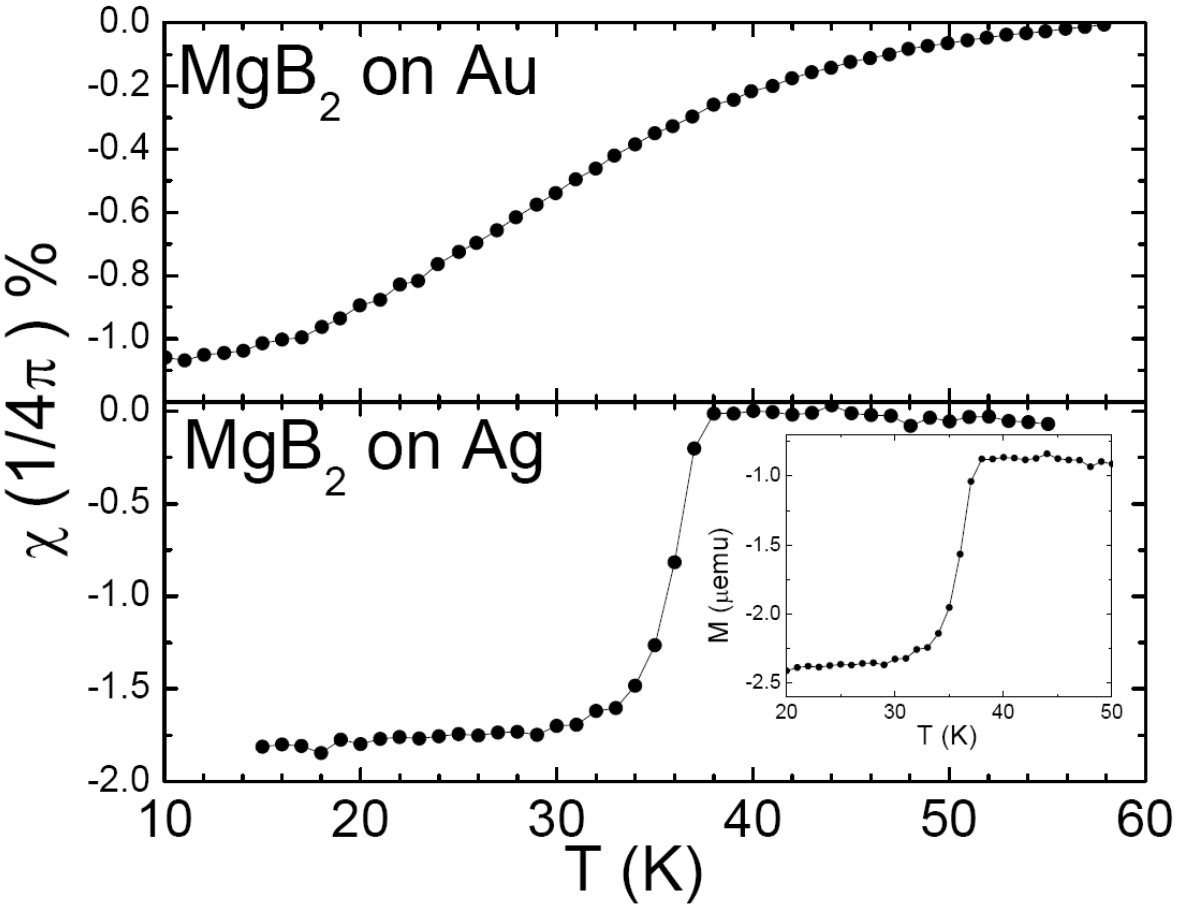

Figure 4.6 (a) Magnetic susceptibility, plotted in units for a perfect diamagnetic, for MgB_2 deposited on an Au substrate, (b) Magnetic susceptibility for MgB2 deposited on an Ag substrate. Inset: Net measured magnetic moment for MgB_2 on Ag with no background correction.

4.3.2 Silicon

The temperature dependence of magnetic susceptibility for MgB_2 on silicon deposited through an alkaline medium is dominated by strong diamagnetic signal and sharp drop at superconducting transition of 40 K at zero magnetic field. The figure 4.6 plots the magnetic susceptibility of samples measured at 0 T (bottom curve), 0.25 T, 0.50 T and 1 T (upper curve). The phase transition is sharp and has a width of $\Delta T = 3.5$ K, thus showing a minimal broadening of superconductivity. The transition temperature decreases monotonically with increasing field. The suppression is very similar to that observed in bulk MgB_2. Using the relative decrease in susceptibility at superconducting transition; we can estimate the superconducting volume in these films. At 10 K fraction reaches 1.3% at low fields but falling to 1.1% in a field of 1T. This is consistent with the presence of impurities in these films together with the high concentration of structural defects. In addition to determining the magnetic measurements we also looked at procuring resistivity data. We were unable to observe any change in conductivity of these samples. This is due to small superconducting fraction which falls below percolation threshold. If the volume fraction is increased by factor of 2 we definitely expect to observe some resistive transition.

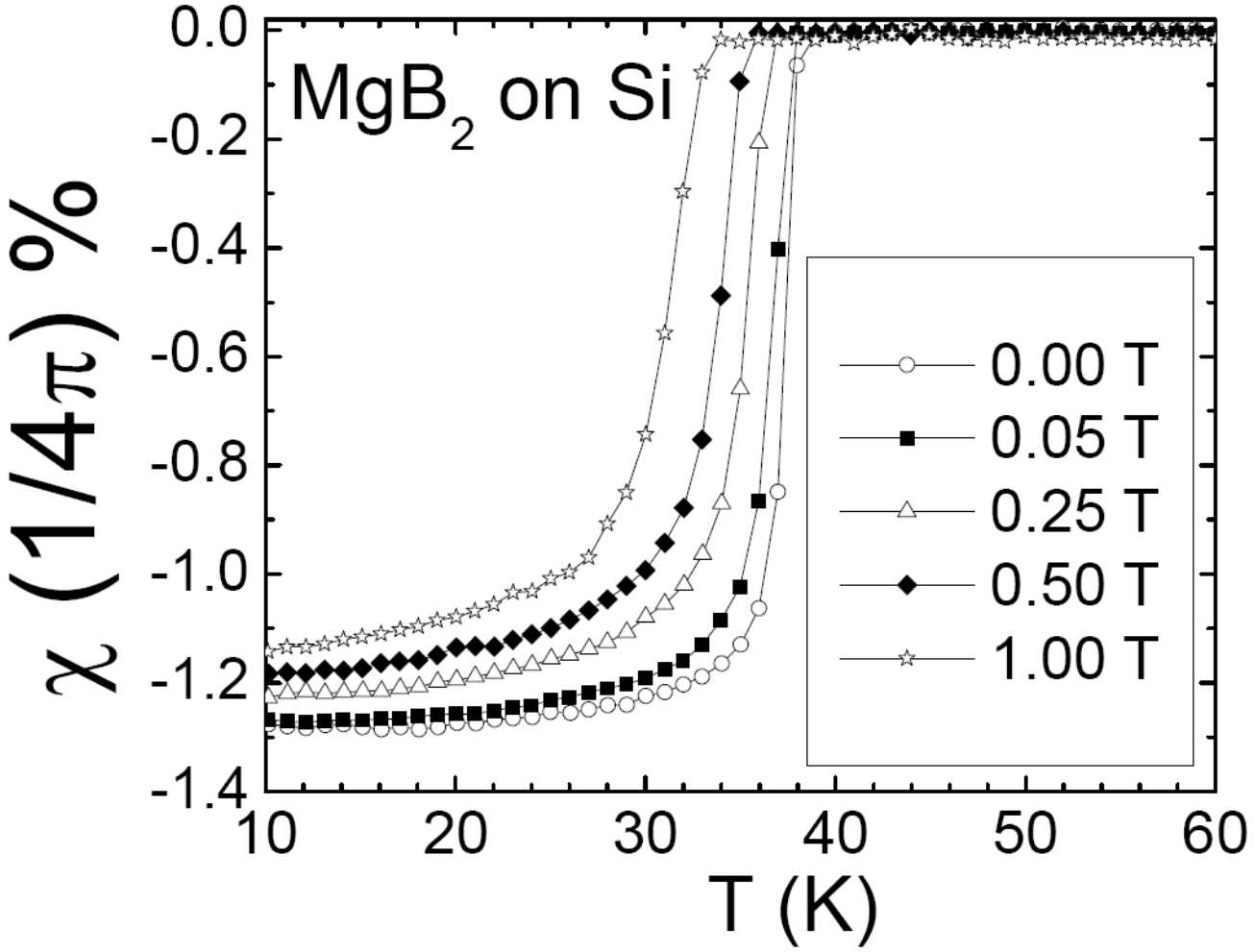

Figure 4.7 Magnetic susceptibility of MgB_2 deposited on Si measured at different magnetic fields, as indicated.

In previous studies we prepared a superconducting thin film of magnesium Diboride on copper which exhibited a film with a very small superconducting volume fraction. However, the results of MgB_2 film deposition on silver and gold show a magnitude increase in superconducting fraction. This improvement in our study is owing to better redox potential values observed in case of silver and gold compared to copper substrate. The poor film quality on copper was due to its easily oxidizing tendency during the deposition process, preventing its activation on substrate surface essential for electroless plating. The theory of controlling the redox potential was also proved through our electroless deposition on silicon. Our previous study provided ineffective results for electroless deposition using conventional acidic electrolytic bath, so we carried out experimental studies of MgB_2 deposition using alkaline electrolytic bath, which were successful as explained in our earlier sections.

In the acidic electrolytic bath the hypophosphite is reduced to H_2PO_{3-} by the following reaction.

$$H_2PO_2^- + H_20 \longrightarrow H_2PO_3^- + 2H^+ + 2e^- \quad (1)$$

The measured redox potential of the bath was 0.499 volt.

Conversely, in the alkaline bath the hypophosphite is reduced to HPO_3^{2-} by the reaction as follows

$$H_2PO_2^- + 3OH^- \longrightarrow HPO_3^{2-} + 2H_2O + 2e- \quad (2)$$

The measured redox potential of the bath was 1.57 volt.

These reactions show that the hypophosphite anion is a much more powerful reducing agent in basic solutions than in acid solutions. This reduction of the hypophosphite ion contributes to the increased redox potential. This drives the deposition reaction of MgB_2 on silicon surface. This higher redox may also reduce surface oxidation at the silicon surface.

4.4 Raman Spectra

We used Raman spectroscopy to probe the microstructure of these thin films using Horiba spectrometer and 514.5 nm green laser as incident light. The Raman spectrum was carried out at many different points across the films, are identical to the shown in Figure 4.7. A factor group analysis yields the decomposition of the coordinate representation for MgB_2 (space group P6/mmm z=1) $G=B_{1g} + E_{2g} + E_{1u} + A_{2u.}$ Of the zone centre optical models, the A_{2u} mode (B and Mg planes moving against each other) and E1u mode (B and Mg planes sliding along *x, y*) are infrared active, the B1g mode (two borons displaced along *z* in opposite directions) is silent, and only the E2g mode (in-plane displacements of borons) is Raman active [31]. We observe the expected E_{2g} Raman active mode at ~620 cm^{-1} for both samples, which is consistent with previous theoretical and experimental studies. We also observed an intense mode at 640 cm^{-1}, which is predicted as MgO complex, an impurity that could be expelled by controlling the redox potential in the electrolytic plating bath during synthesis technique. Apart from MgO there are various other peaks that are also observed that are not attributed to $MgB_{2.}$ Raman data for films prepared on silicon show additional peaks at 300 cm^{-1}, 520 cm^{-1} and 950 cm^{-1} apart from the substrate and MgB_2. These peaks are indications of impurity phases; that are consistent with XRD data that also show secondary phases present on films. Most of these impurities are present in our bulk precursor material as proven in Raman data (not shown) for bulk $MgB_{2.}$ The data obtained was identical and consistent due to structural uniformity of the films.

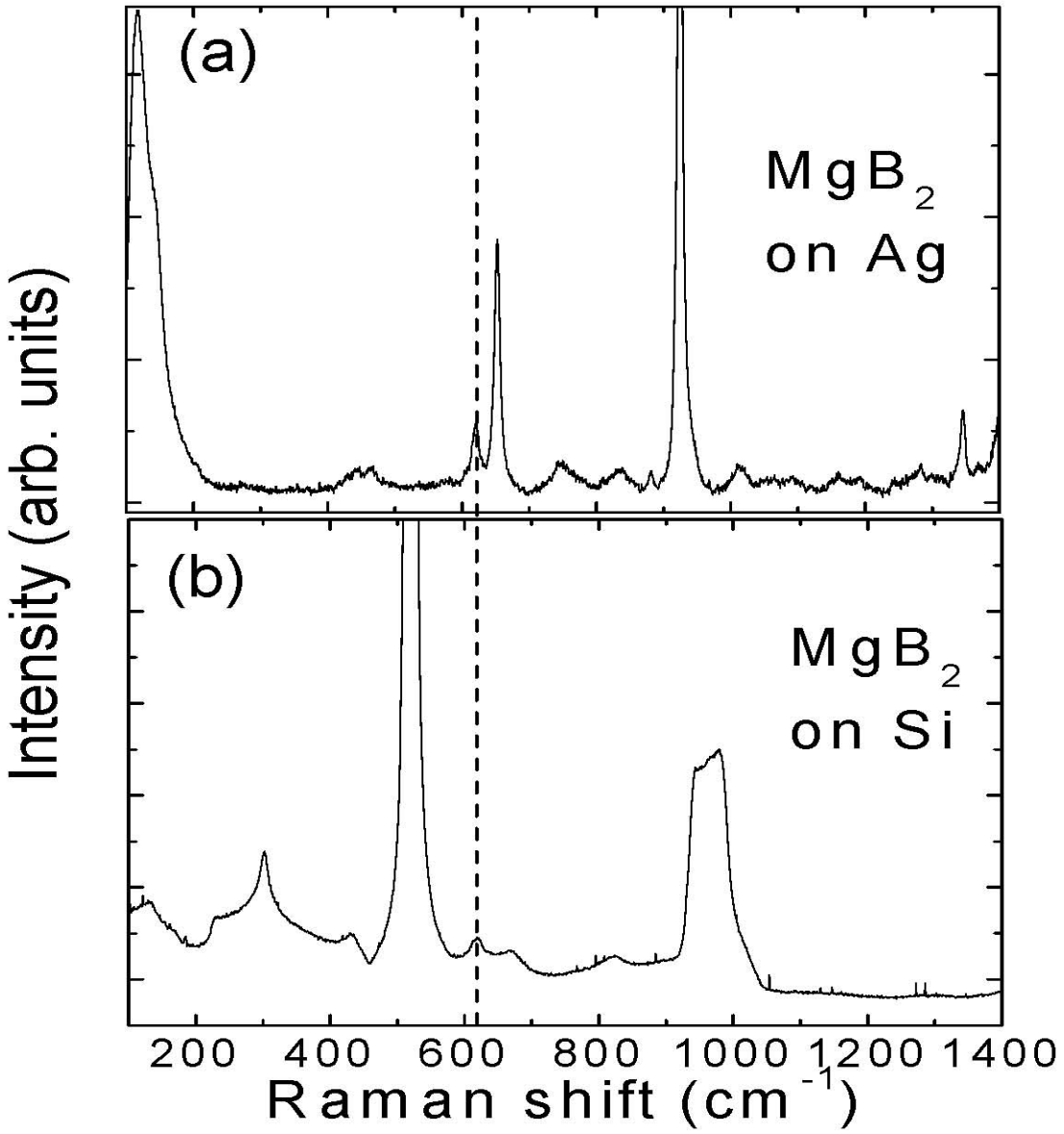

Figure 4.8 (a) Raman spectrum for MgB_2 deposited on Ag, (b) Raman spectrum for MgB_2 deposited on Si. The dashed line indicates the 620 cm^{-1} peak expected for MgB_2

CHAPTER 5 - CONCLUSIONS

1. MgB_2 films were deposited on to conducting and non-conducting substrates using a novel electroless deposition technique. This study extended previous investigations of lower quality films prepared on copper to develop an approach to synthesizing films on silver, gold and copper. The three metals have very high electrical conductivity, with the conductivity of Silver being $63.0*10^{-6}$ S/m, Copper $59.6 * 10^{-6}$ S/m, and Gold $45.2*10^{-6}$ S/m. These values emphasize the importance of copper, in particular, for electrical application due to its electrical properties and low cost.

   The deposition of MgB_2 onto any non-conducting substrates, such as silicon, had not been done successfully in the past The ability to use electroless deposition to prepare MgB2 on Si greatly expands the potential applications for this system due to the wide industrial use of Si in semiconductor devices, integrated circuits and microchips.

2. This study represents the first time that the electroless deposition of any compound was successfully achieved. This technique is conventionally only used to deposit metals, such as: Nickel, Aluminum, or Copper. The deposition of the compound MgB_2 deposition proceeds through reactions due to the ionization of water at the substrate surface and coordination of hydroxyl ions to obtain magnesium and boron ions on the active surface.

3. The MgB2 films were prepared on silver and gold using an acidic electrolytic plating bath. The films on silver show a sharp superconducting transition at 38 K; gold exhibits a rather broad transition just below 40 K. The temperature dependence of the critical field was also similar to that of bulk MgB_2 and the samples had superconducting fractions of 2% for silver and 1% for gold. The diamagnetic signal in these samples is much higher

than found in previous MgB2 films on copper, which developed a superconducting volume fraction of only0.1-0.2 %. This significant improvement in superconducting quality represents an important advance in our research studies. In our future work we will need to achieve still larger superconducting fractions, which may be accomplished by depositing more uniform and more homogeneous films. This may be accomplished by varying the deposition parameters or adjusting the treatment of as-deposited film.

4. The films on silicon were prepared using an alkaline electrolytic plating bath. The superconducting transition was observed at 40 K at zero magnetic fields. On the application of higher magnetic fields the transition temperature decreased monotonically to 34 K at 1 Tesla. The alkaline plating bath minimized the oxidizing tendency for silicon substrate unlike so in acidic plating bath. This investigation emphasized the importance of controlling oxidation potential, which was not realized in previous investigations.

5. XRD studies confirmed the presence of polycrystalline MgB_2 along with some secondary phases. The SEM cross sectional study showed that the film thickness on silicon was 13 μm compared to 1μm on conductive substrates such as silver. There remains an analysis on how this could be achieved when the silicon has fewer catalytic site compared to surfaces on silver and gold. Another open question also remains concerning the relation between the film thicknesses and superconducting properties, as magnesium diboride crystals are extremely brittle and tend to crack above a threshold thickness. The SEM images show cracks in the film that may arise from differences in the thermal expansion between the substrate and film. This cracking will need to be eliminated through more effective annealing procedures especially controlling the rate of cooling and heating.

6. The Raman spectrum shows an active mode at 620 cm^{-1}, consistent with theoretical predictions for MgB_2. The Raman spectra also show peaks at certain other modes that are similar to those observed in bulk MgB_2 powder, thus proving presence of impurities in precursor materials

7. Results obtained show evidence of MgB_2 formation by electroless deposition with presence of oxide and magnesium segregation, which may explain the low quality of these samples. These compounds are present in the as-deposited films, and the annealing process tends to segregate impurities near the surface of film.

8. The temperature dependent resistivity for these superconducting MgB_2 films could not be measured on any of the samples. Resistivity measurements require uniform deposition without presence of cracks as present on figures shown in our results and discussions.

9. The world's requirement of power is increasing daily and in time it will reach capacity and grid will not be able transfer any more power. Replacing them with superconducting wires will be a good way forward. Superefficient, environmentally friendly motors and underground transmission lines can revolutionize the power grid. Superconducting wires have large scale applications in motors, power cables and high strength magnets as well. The conventionally used superconducting wires now are Niobium-Tin alloy. Magnesium Diboride with a higher Tc than Nb-Sn can reduce refrigeration cost and with effective uniform deposition on curved surfaces such as wire using electroless plating technique; it can boost performance with good mechanical property and high engineering critical

current density in applied magnetic field. This can very well revolutionize and broaden the scope & application of superconducting wire industry.

REFERENCES

1. A.B. Jadhav, and S.H. Pawar, "*Electrochemical synthesis of superconducting magnesium diboride films: a novel potential technique*". Superconductor science & technology, 2003. **16**: p. 752-759.
2. Y.B. Zhu, et al., "*Fabrication of MgB_2 superconducting thick films by electrophoresis technique*". PHYSICA C, 2002. **371**(1): p. 7-9.
3. M.B.A.P Nath, "*A Simple Sol-Gel Synthesis of Superconducting MgB_2 Nanowires*". Advanced Materials, 2006. **18**(19): p. 2504.
4. K. Ueda, and M. Naito, "*As-grown superconducting MgB2 thin films prepared by molecular beam epitaxy*". APPLIED PHYSICS LETTERS, 2001. **79**: p. 2046-2048.
5. N. Peng, et al., "*Ion beam synthesis of superconducting MgB2 thin films*". APPLIED PHYSICS LETTERS, 2003. **82**: p. 236-238.
6. S.F. Wang, et al., "*Superconducting MgB2 Thin Films with T_c of about 39K Grown by Pulsed Laser Deposition*". 2001. http://arxiv.org/abs/cond-mat/0104555.
7. F.M. Donahue, and Yu, C. U., "A Study of the Mechanism of the Electroless Deposition of Nickel," *Electrochim. Acta*, Vol**.**15, pp.237, 1970.
8. Glenn O Mallory, "Electroless plating – Fundamentals and Applications", Chapter 2, The Electroless Nickel Plating Bath- Effect of Variables on the Process", Edited by: O. Glenn Mallory, Juan B. Hajdu, B. June, Sponsored and Published by the American Electroplater's and Surface Finisher's Society, pp. 193, 201, © 1990 William Andrew Publishing/Noyes.
9. Perminder Bindra and James R. White, Electroless plating – Fundamentals and Applications", Chapter 12, "Fundamentals of Electroless Copper Plating" Edited by: O.

Glenn Mallory, Juan B. Hajdu, B. June, Sponsored and Published by the American Electroplater's and Surface Finisher's Society, pp. 289,290, 1990

10. V.R. Nagarajan, P.R. Kharel, S. Putatunda, G. Lawes, "*Synthesis and characterization of superconducting lead films by electroless plating on metallic and non-metallic substrates*", Materials Science and Engineering B Vol 151, pp 191-195 (2008).
11. V. R. Nagarajan, S.K. Putatunda, P.R. Kharel, G. Lawes, "*Synthesis of superconducting thin films of magnesium diboride by electroless plating*", Materials and Manufacturing Processes Vol 24, 633 - 638 (2009)
12. Kristian Fossheim and Asle Subdo, Superconductivity: physics and its applications. P.cm
13. P.W Atkins, Physical Chemistry 6 ed.1998 Oxford University Press p. 621
14. D.P.Michael Cyrot, Introduction to superconductivity and high T_c materials 1 ed. 1992 World Scientific publishing Co.Ltd.
15. C.Whelan, BCS Theory of superconductivity in Quantum Mechanics for Engineers 2003.
16. Rod Nave, Introduction to hyper-physics: Exploring physics and astronomy in neutral net type environment, Georgia State University
17. D. Pines, Understanding high temperature superconductivity – Progress and prospects 1997. 11(19): p. 12-14
18. Neeraj Khare, Ray Radenbaugh, V.I.Shnyrkov, Shoji Tanaka, A.Ya.Tzalenchuk, "Handbook of high temperature superconductor electronics", p. 1- 12, Copyright 2003, by Mercel Dekker Inc.
19. J.G. Bednorz, K.A.Mueller, Possible high T_c superconductivity in Ba-la-Cu-O system, Z.Phys, B. Condensed Matter 64:189-193, 1986

20. J. Nagamatsu, et al., "*Superconductivity at 39 K in magnesium diboride*". Nature, 2001. 410 (6824): p 63-64

21. D.K.F.P.C Canfield, S.L. Bud'ko, J.E. Ostenson, G.Lapertot, C.E.Cunnigham and C.Petrovic, Superconductivity in $MgB_{2,}$ Physics Review Letters, 2001. 86: p 2423

22. C.B.T Yamashita, The Origin of Multiple Superconducting Gaps in $MgB_{2,}$ Superconducting Science Technology, 2001. 14: p.115

23. W.N.Kang, H.J.Kim, E.M.Choi, C.U.Jung, S.L.Lee. MgB_2 Superconducting Thin Films with a transition temperature of 39 K Science 2001: 292: p. 1521-1523.

24. Parminder bindra, David Light, David Rath. Mechanism of electroless metal plating 1: Mixed potential theory and interdependence of partial reactions Journal reference and IBM copyright, Vol 28 No.6 1984

25. N.Petrov, Y.Sverdlov and Y.Schaham-Diamand, Journal of Electrochemical Society 149 C187, Electrochemical study of electroless deposition of Co(P) and Co(W,P) alloys

27. Paul Szymanowski, Micro plating Inc. http://www.corrosion- doctors.org/MetalCoatings/Electroless.htm

28. Brad Durklin,"Controlling nickel plating bath", McDermid Inc. Waterbury, The web resource for product finishing professionals. Gardner Publication 2008

29. Ridel W, "Electroless nickel plating" ASSM International-finishing publications LTD. 1981

30. Mordechay Schlensinger, Electrochemistry Encyclopedia, Wiley, New York, 2002

31. Lei Shi, Huarong Zhang, Lie Chen and Yong Feng. The Raman spectrum and lattice parameters of MgB_2 as a function of temperature, Journal of physics matter: condensed Matter 16, 2004

ABSTRACT

ELECTROLESS DEPOSITION OF SUPERCONDUCTING MAGNESIUM DIBORIDE THIN FILMS ON VARIOUS SUBSTRATES

by

KHRUPA SAAGAR VIJAYARAGAVAN

MAY 2010

Advisor: Dr. Susil K Putatunda
Dr. Gavin Lawes

Major: Chemical Engineering

Degree: Masters of Science

Superconducting thin films of magnesium diboride were synthesized by a novel electroless plating process. Electroless plating shares many similarities to electroplating with the major difference being the absence of a continuous bias voltage. Significantly, this work represents the first investigation where electroless deposition has been used to prepare compounds, as opposed to the elemental metals considered in all previous studies. Magnesium Diboride is a recently discovered superconducting material with a relatively high transition temperature (T_c = 39 K). MgB2 plated wires offer potential applications for MRI (magnetic imaging resonance), NMR (nuclear magnetic resonance), particle accelerators and the electronic industry. The low cost and wide availability of magnesium diboride make this material a possible future source of superconducting magnets to replace the Nb-Sn (Niobium Tin) alloy that that is presently used. The MgB_2 thin films were synthesized on conducting substrates including silver, gold, copper and insulating silicon. Thin solid film deposition is widely used in the electronic industry for benefits in high power storage, transmission and

low power consumption. In this electroless plating of $MgB_{2,}$ sodium hypophosphite was used as a reducing agent in acidic and alkaline plating solutions. The structural, morphological and superconducting properties of these films were examined using X-ray diffraction, temperature-dependent magnetometry, scanning electron microscopy (SEM), energy-dispersive X-ray analysis (SEM-EDX) and Raman spectroscopy. The magnetic study of these thin films indicates the presence of clear superconducting phase below the critical temperature of roughly 39K with a diamagnetic susceptibility corresponding to approximately 1-2% of a perfect superconductor for different substrates. The vibrational spectroscopy of these thin films confirms the crystalline nature and correct stoichiometry of $MgB_{2.}$ The structural and microstructural analysis of these thin films indicates the polycrystalline nature of the film with presence of small amount of impurity phases of different magnesium and boron compounds. The SEM analysis also determines the cross sectional thickness acquired on substrate surface. The synthesis process of these films and their superconducting properties will be discussed in detailed.

AUTOBIOGRAPHICAL STATEMENT

Khrupa Vijayaragavan is a second year graduate student completing a Masters in Chemical Engineering. He received his B.S in Chemical Engineering from R.V. College of Engineering, Bangalore, India in July 2006. Khrupa's research has been principally focused on developing new techniques for electroless deposition, with a specific emphasis on preparing superconducting compounds.